Heliyon 7 (2021) e06342

Contents lists available at ScienceDirect

Heliyon

journal homepage: www.cell.com/heliyon

Research article

Application of soft-computing techniques for statistical modeling and optimization of *Dyacrodes edulis* seed oil extraction using polar and non-polar solvents

C. Esonye [a,*], O.D. Onukwuli [b], V.C. Anadebe [a], J.N.O. Ezeugo [c], N.J. Ogbodo [a]

[a] Department of Chemical Engineering, Alex Ekwueme Federal University, Ndufu-Alike, Abakaliki, Nigeria
[b] Department of Chemical Engineering, Nnamdi Azikiwe University, Awka, Nigeria
[c] Department of Chemical Engineering, Chukwuemeka Odumegwu Ojukwu University, Uli, Nigeria

ARTICLE INFO

Keywords:
Dyacrodes edulis
Modeling
Optimization
Solvent extraction
RSM
ANN-GA

ABSTRACT

This research presents optimal factor evaluation for maximum *Dyacrodes edulis* seed oil (DESO) extraction by applying central composite design (CCD) based on Box-Behnken (BB) experimental design of response surface methodology (RSM) and Artificial neural network (ANN) on feed forward-back propagation (FFBP) of Levenberg Marquardt (LM) training algorithm. Polar solvents (ethanol and combination of methanol and chloroform (M/C)) and non-polar solvents (n-hexane) were used for the extraction. The RSM optimal predicted oil yields were 45.21%, 38.61% and 30.87% while experimental values were 46.01%, 40.71% and 32.45% for n-hexane, ethanol and M/C respectively. The RSM optimum conditions were particle size of 450.67, 451.19 and 450.22μm, extraction time of 55.57, 55.16 and 56.11min and solute/solvent ratio of 0.19, 0.16 and 0.18 g/ml for n-hexane, ethanol and M/C respectively. The ANN-GA optimized conditions showed 5.14, 5.81 and 2.12 % higher DESO yields at 1.10, 0.26 and 0.65% smaller particle sizes, 5.47, 0.30 and 0.62 % faster extraction rate, and 24, 11.11 and 10% more solute requirement, for n-hexane, ethanol and M/C solvents respectively. The particle size was found to be the most significant factor. ANN and RSM established good correlations with the experimental data but ANN showed higher predictive supremacy than RSM based on its higher values of R^2 and lower error indices. Also, ANN-GA provided more economical optimal DESO extraction route. The physico-chemical characteristics, functional groups and fatty acid compositions of the seed oil compared with literature values and suggest high commercial values for DESO. Therefore, the obtained results present a viable method to harness the useful and highly potential seed oil from *dyacrodes edulis* for many industrial applications.

1. Introduction

Vegetable oil is basically water–insoluble and hydrophobic substance in plants that are made up of one mole of glycerol and three moles of fatty acids and are commonly referred to as triglycerides. The fatty acids vary both in carbon chain length and in number of unsaturated bonds (Fangrui and Hanna, 1999). Vegetable oil could be obtained from various parts of plants but more in abundance in either the fruit mesocarp or fruit seed. However, vegetable oil could be either edible (rape seed, soybean, peanut, sunflower, palm and coconut oil) or non-edible (*jatropha, karanja*, sea mango, algae and halophytes) (Aiwize and Achebo, 2012; Atabani et al., 2012). Many commercial applications of vegetable oil exist for improvement of socio-economic well being of man. The above applications are challenged by food-fuel crises and in ability to meet up with the industrial demands (Atabani et al., 2012). It is currently reported that there are more than 350 potential oil bearing crops with high oil content for various domestic and industrial uses in the world (Esonye et al., 2019a). Palm oil dominates the global vegetable oil market with over 73 million metric tons in 2020 (Statista, 2020; Global vegetable-oils-Business-Report 2018). Extensive researches on how to effectively harness the widely distributed seed oils to enhance large scale production and match the global consumption rate is therefore necessary.

Most methods of vegetable oil extraction seem to be very costly due to inability to control some inherent factors such as long process time and post extraction treatment (Atabani et al., 2012; Achten et al., 2008). A lot of researches have been carried out to find alternative ways of producing oil for process industries and for food industry (Uzoh and Onukwuli, 2016). Solvent extraction by sohxlet has been reported to be most

* Corresponding author.
E-mail address: esonye.chizoo@funai.edu.ng (C. Esonye).

https://doi.org/10.1016/j.heliyon.2021.e06342
Received 8 November 2020; Received in revised form 13 January 2021; Accepted 18 February 2021

efficient technique (Topallar and Gecgel, 2000) that leaves a residue of less than 1% oil (Ochigbo and Paiko, 2011). Solvent extraction is the technique of removing one constituent from a solid by means of a liquid solvent. It is also called leaching and has the most industrial application among all the oil extraction methods. There are three methods that are used in solvent extraction and they are: hot water extraction, sohxlet extraction and ultrasonic technique. Musa et al. (2015) studied the effect of process variables (particle size, temperature and time) using ethanol as solvent but did not vary the solvent used in the oil extraction from the seeds of *Chrysophyllium albidium*. Tsakins et al. (1999) used n-hexane and mixture of chloroform/methanol in *Moringa olifera* seed oil extraction and obtained 35.7% and 31.2% oil yields respectively. Also, Igbum et al. (2012) extracted palm kernel oil (PKO) using solvent extraction method and a yield of 42.0 % was achieved.

There are many factors influencing the rate of extraction by solvent extraction method such as particle size, solvent nature, and temperature and agitation rate. The seeds are preferred to be reduced to smaller particle sizes through milling to facilitate the release of more oil from cell of the seed. It ensures more surface area for solvent-solute contact, faster and easier infiltration of transfer media and reduces the length of solvent diffusion path for high oil yield to be achieved. Polar solvents that were commonly studied were acetone, ethyl acetate, iso-propanol and ethanol while n-hexane has remained the non-polar solvent of most interest by previous authors (Adebayo et al., 2012; Bello et al., 2011). N-hexane has been applied by several researchers because of its ability to extract high amount of oil from plant seeds (Giwa and Ogunbona, 2014; Betiku and Adepoju, 2013). Also, other reasons why non-polar solvents like hexane are preferred in many cases are due to their many superior attributes such as: simple recoveries, low latent heat of vaporization (330 kJ/kg), narrow boiling point range (63-69 °C) and high solubility. Notwithstanding, their application gives serious concerns on health, safety and environment (Dash et al., 2017) and consequently classified as hazardous (Castejon et al., 2018). Polar solvents are considered because they are non-inflammabe, widely distributed, thermally stable and possess low vapour pressure (Chemat et al., 2019). Also, most of them are naturally occurring and derived from agro-waste (Kumar et al., 2017).

However, most previous reports on oil extraction lacks statistically optimized conditions that could serve as optimal routes for industrial scale up. Therefore, there is need for process industries to optimize current methods of oil extraction to ascertain their viability and feasibility which has resultant effect of achieving high profits. Consequently, researches on oil extraction is currently directed towards the application of soft-computing techniques and artificial intelligence tools to save time, energy and resources which equally help to establish standard operating procedures in the oil solvent extraction processes. Therefore, the application of statistical optimization techniques such as response surface methodology (RSM), artificial neural networks (ANN), adaptive neuro-fuzzy inference system (ANFIS) and their integration with genetic algorithm to provide optimal routes for solvent extraction of oil from seeds has become very necessary and is currently receiving great attention (Ropo et al., 2020). D-optimal design has been extensively applied in the optimization of the oil extraction from *moringa oleifera* (Oladipo and Betiku, 2019), rubber seed (Ropo et al., 2020) and *hura crepitans* (Paul et al., 2019). Also, comparative analysis of the capability of RSM and ANFIS-GA as well as ANFIS/ANN on predicting the oil yield from *hura crepitans* has been studied (Ropo et al., 2020; Nwosu-Obiegu et al., 2020). The application of RSM and ANN for the optimization of oil extraction from *gmelina* (Uzoh and Onukwuli, 2016), lucky nut (Adepoju et al., 2018) and *hevea brasiliensis* (Onoji et al., 2017) has equally been reported. It is therefore, evident that although previous researches have proven that the RSM and ANN-GA techniques are always complimentary (Betiku et al., 2018), the comparative assessment of RSM and ANN-GA for oil extraction has scarcely been reported. Also, the applications of methanol and chloroform as polar solvents have not been statistically optimized. RSM has the flexibility, robustness and capability to navigate design space, establish optimum conditions and minimize the number of experimental stages required to provide adequate and efficient result (Esonye et al., 2020). Also, ANN is a widely recognized evolutionary computation method with great ability in resolving complex nonlinear systems and control problems. Since response surface methodology has inbuilt desirability function and numerical optimization tool that is lacking in ANN application, integrating ANN with genetic algorithm is one of the best approaches to harness ANN best potential, achieve optimal conditions for desired responses and create best conditions for effective comparison between RSM and ANN as optimization tools.

Interestingly, the seed oil from *dyacrodes edulis* seed (DES) has been established as sustainable material for renewable energy with high commercial value and industrial potential (Esonye et al., 2019b). Unfortunately, its extraction process has not been optimized. *D. edulis* is a perennial fruit tree that is indigenous to West Central Africa and Gulf of Guinea and has about 48% oil in the fruit pulp with a hectare of its plantation yielding about 8 tonnes of oil (Esonye et al., 2019c). The seed contains high saturated fatty acids made up of over 50% oleic acid with impressive high oil content of over 40wt% (Esonye et al., 2019a). However, this seed is thrown away as waste after consuming the juicy pulp (Esonye et al., 2019c). The justification for the selection of the solvents in this study is that n-hexane has been widely established as having the ability to extract high oil from seed meal and require less energy, ethanol is biodegradable and has renewability potential while methanol/chloroform are cheap and non-polar solvents that have the ability to overcome forces that hold the fats within the sample matrix (Lalas and Tsakins, 2002). Therefore, this study tends to present optimal conditions for the solvent extraction of *dyacrodes edulis* seed oil (DESO) by utilizing the complimentary advantages of RSM and ANN-GA. The applications of Fourier transform infrared (FTIR) and gas chromatography mass-spectrometry (GCMS) and the Association of Official Analytical Chemists (AOAC) standard methods for characterization of the extracted oil are equally reported.

2. Materials and methods

2.1. Materials

All the analytical grade reagents and chemicals were obtained from popular Bridge-Head Chemical market in Onitsha city, Nigeria. The fresh and matured fruits of *dycarodes edulis* (African pear) (Figure 1) were harvested from Osoala-Umueme Ngwaobi in Isiala Ngwa South L.G.A of Abia state, Nigeria. The location is between latitude 5° 06′ 23.69N and longitude 7° 22′ 0.01E. The matured *D. edulis* fruits were washed several times with water before cutting, opening and separating them into seeds and pulp. The clean seeds were dried under the sun for 1 week before being crushed into meals using electric milling machine. The composite meal was further sun dried for a period of 5 days to remove residual moisture and latter sieved using ASTEM 11–70, EML 200- Haver-Boecker apparatus to obtain different particle sizes (200, 300, 400, 500, 600 and 700 μm).

2.2. Oil extraction

The seed meal from each individual sample were extracted by n-hexane (95% purity), ethanol (99% purity) and methanol/chloroform (50:50) (>99% purity) solvents (Keneni et al., 2020; Tsakins et al., 1999). The solvent extraction process was carried out using 200ml soxhlet apparatus. About 20g of the ground meal of a particular particle size was subjected individually to the solvent extraction for a particular time duration as contained in Table 1 and temperature of 69 °C, 78 °C and 70 °C for hexane, ethanol and methanol/chloroform solvents respectively (Keneni et al., 2020). The oil solutions were filtered and subjected to distillation using rotary evaporator. Oil degumming was done by adding 3 wt% of warm water and mechanically agitating the mixture with magnetic stirrer for about 30 min at a temperature of 60 °C. This helped the emulsifiers to separate from the oil with ease (Ofoefule

Figure 1. African pear fruit, (a) Fruit, (b) Seed, (c). released seed for drying and (d) ground seed.

Table 1. Independent variables in the experimental plan of Box-Behnken for DESO extraction.

Variables	Symbols	Coded levels		
		-1	**0**	**1**
Particle size (μm)	X_1	300	400	500
Extraction time (min.)	X_2	45.00	52.50	60.00
Solute/solvent ratio (g/ml)	X_3	1:4	1:5	1:6

et al., 2019). The refined oil was separated from the emulsifiers and water by decanting after settling by gravity. The separated oil was oven dried for 1h to remove residual moisture. Finally, the percentage oil yield was determined as stated in Eq. (1).

$$\text{DESO } (\text{wt}\%) = \frac{W_o}{W_{sm}} \times 100 \quad (1)$$

where, DESO is the *dyacrodes edulis* seed oil yield

W_o is the weight of refined oil in g
W_{sm} is the weight of the seed meal used in g

2.3. Physico-chemical characterization of the oil

The physico-chemical characterization of the extracted seed oil was done by determining the acid value, saponification value, peroxide value and iodine value based on Association of Official Analytical Chemist

method (AOAC, 2000). Also, other properties of the extracted oil such as viscosity, specific gravity and moisture content were ascertained using Oswald viscometer, density bottle and oven method respectively. The flash point was ascertained using American Standard for Testing and Materials (ASTM D.2500). All the analyses carried out on the physico-chemical parameters of the oil were carried out in triplicates and the average values and standard deviations were calculated and presented.

2.4. FT-IR analysis of the oil

Fourier transform infra red (FT-IR) analysis was performed to ascertain the functional groups present in DESO using IR Affinity-1 Shimadzu, model No: 3116465. The DESO sample was introduced through sample cell while cleaning of the cell was done with tri-solvent mixture of acetone-toluene-methanol prior to background collection. An aliquot of 0.5ml of the sample (DESO) was taken using the sample cell and introduced into the cell unit of the system. The scan results were obtained as spectra from microlab software attached to supporting computer system. The peaks of the spectra obtained were identified and interpreted to identify the functional groups in the molecules of the DESO (Esonye et al., 2019a).

2.5. GC-MS analysis of the oil

The fatty acid composition of the biodiesel samples were ascertained in accordance with AOCS official method Ce 2–66 using GCMS-QP2010 plus, Shimadzu. GC-MS was preferred in this study because it is faster than the GC, provides molecular weight information and requires an aliquot sample. The GC-MS fragments the analyte to be identified on the basis of its mass and the column was calibrated by introducing standards while dilution of the sample in a little quantity of ethyl acetate was done to achieve excellent separations. Hydrogen served as the carrier gas and its flowrate was controlled at 41.27 ml/min while the flowrate of the column was set at 1.82 ml/min. The oven temperature was fixed at 80 °C before increasing up at 6 °C/min and then up till 340 °C. The Peaks identification was done using Mass Spectra Library (Fu et al.,2008).

2.6. DESO oil extraction optimization and modeling

2.6.1. Experimental design and statistical analysis by RSM

A standard response surface methodology design called Box-Behnken design of experiment (BBDE) was applied to develop the standard combinations of the process conditions for maximum oil extraction from the seed of *dyacrodes edulis*. BBDE is a rotatable design that usually generates higher order response surfaces using fewer required experimental runs than normal factorial design (Das and Dewanjee, 2018). It was designed by George E. P. Box and Donald Behnken in 1960 to ensure that each factor or independent variable is placed at one of the three equally spaced values and at least 3-levels are required. The design can be sufficient to fit second-order model including the squared effects and interactive factors. Reasonable ratio of the number of experimental points to the number of coefficients in the quadratic model is achieved. It applies twelve middle edge modes and three centre modes to fit a second-order polynomial equation. It does not depend on full or fractional factorial designs. Considering this study, for a three factors requiring three levels (particle size, extraction time and solute solvent ratio), the points are located in the middle of the edges of the experimental domain as shown in Figure 2. The design has the great advantage of reducing the experimental runs from 20 (if central composite design was used) to 17 runs. The main objective of this experimental design was to investigate the interactive effects of the oil extraction variables and to optimize the oil yield from the tested variables. Linear, quadratic, and cross-product effects of the process variables on the percentage oil yield were studied. Recently, much attention has been given to extraction time, solid/solvent ratio and solvent type or nature of solvent with little or no consideration to solute

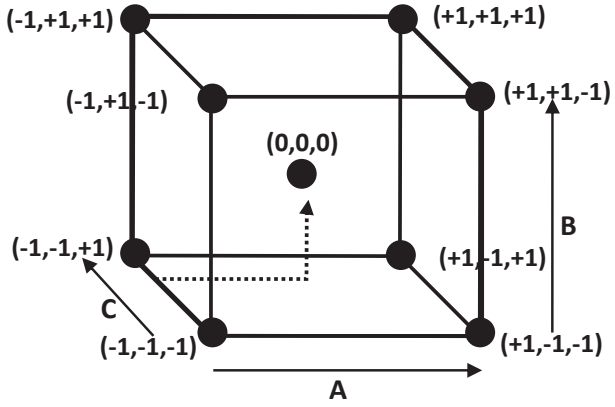

Figure 2. A graphical representation of Box-Behnken design.

particle size (Mwaura et al., 2020; Obiegu-Nwosu et al., 2020). Therefore, particle size (X_1), extraction time (X_2) and solute/solvent ratio (X_3) were identified as the set of independent variables with their ranges selected based on preliminary studies (Adepoju et al., 2018). The selected process variables units, notations and limits are presented in Table 1 based on preliminary reports (Ropo et al., 2020).

The model fit was carried out by calculating the significance of each type of model. The sum of squared error (SSE), root mean squared error (RMSE), the R-squared and adjusted-R squared were determined for linear model (LM), linear interactive model (LIM), pure quadratic model (PQM) and quadratic model (QM). The results obtained were used to prove the adequacy of each of model (Ohale et al., 2017). The R^2 is one of the indices used to test the degree of variability between the experimental and predicted responses. The order of fitness of models for n-hexane extraction was found to follow QM > LIM > PQM > LM based on the lowest values of SSE and RMSE and highest values of R^2 (Table 2). The same trend was observed for ethanol and M/C extractions. Therefore, quadratic polynomial equation (Equation 2) as suggested by Zainudin et al. (2016) was selected as the most appropriate model. The process flow chart for the RSM is shown in Figure 3b.

$$Y = \beta_0 + \sum_{i=1}^{n} \beta_i x_i + \sum_{i=1}^{n} \beta_{ii} x_i^2 + \sum \sum_{i=1}^{n} \beta_{ij} x_{ij} \quad (2)$$

where β_0 is a constant, β_i is the linear coefficient, β_{ii} is the quadratic coefficient, β_{ij} is the interactive coefficients, X_i and X_{ij} are the un-coded independent variables and Y is the predicted response (% oil yield). Regression analysis and analysis of variance (ANOVA) were performed using MATLAB 8.5, 2015 version software. The fitted second-order polynomial equations obtained from regression analysis were used to develop the response surface plots.

2.6.2. Development of artificial neural network (ANN) model

The ANN model is developed using MATLAB 8.5 software, 2015 version with a consolidated data set comprising of seventeen (17) data sets for the oil extraction while extraction time, particle size and solute/solvent ratio were used as the input parameters. The back propagation algorithm was used for network training, 70 percent of the data was taken for training set, 15 percent for validation and the remaining 15 percent for the test set in order to assess the generalization and estimation capabilities and the reliability of the ANN model. The ANN training was made more efficient by scaling the inputs and targets data set in the range of -1 to +1. By a trial-and-error approach, the choice of the number of hidden neurons was evaluated. This was achieved by testing different number of neurons until the minimum value of MSE is obtained. The number of hidden neurons chosen resulted in the type of network topology obtained. In this study, a three-layered feed-forward neural network with tangent sigmoid transfer function (tansig) (Equation 3) at hidden layer and linear transfer function (purelin) (Equation 4) at output

Table 2. RSM Model fit summary.

Source/model	SSE	RMSE	R^2	Adj. R^2
LM	114.46	2.97	0.35	0.20
LIM	60.69	2.46	0.66	0.49
PQM	102.13	3.2	0.42	0.28
QM	38.54	2.35	0.80	0.62

LM-Linear model; LIM-Linear interaction model; PQM- Pure quadratic model; QM- Quadratic model.

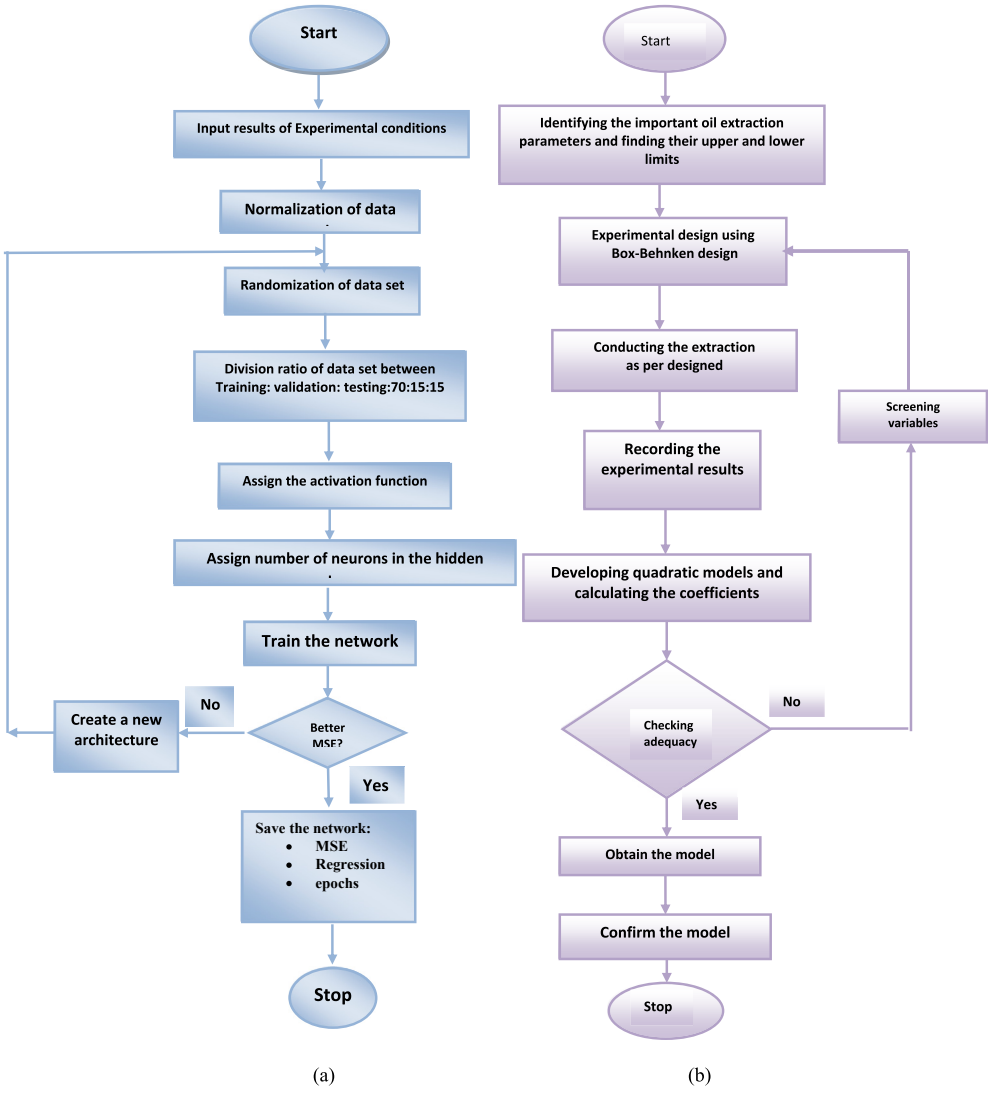

Figure 3. The flowchart of (a) ANN and (b) RSM models development.

layer were used while Eq. (5) represents the activation function. Figure 3a shows the process flow chart for the development of the ANN.

$$X = W^h \mathrm{V} + b^h \tag{3}$$

$$Y = W^{out} \mathrm{f(x)} + b^{out} \tag{4}$$

$$g(t) = tansig(t) = \frac{1 - e^{-t}}{1 + e^{-t}} \tag{5}$$

where X -hidden layer output; V- vector of the network input; W^h - the layer weight, b^h - hidden layer bias; Y- network output, W^{out} - output layer weight; b^{out} - output layer bias; g(t) - activation function.

2.7. ANN-GA optimization

The ANN model was coupled with genetic algorithm (GA) tool kit in MATLAB 8.5, 2015a version to optimize the oil yield. Genetic algorithms are class of evolutionary algorithms that use techniques inspired by evolutionary biology such as inheritance, mutation, selection, and crossover or recombination. The evolution normally begins from a population made up of randomly generated individuals and happens in generations. In each generation, the fitness of every individual in the population is evaluated; multiple individuals are chosen from the current population based on their fitness, and modified to form a new population. Flowchart of how the genetic algorithm was applied is

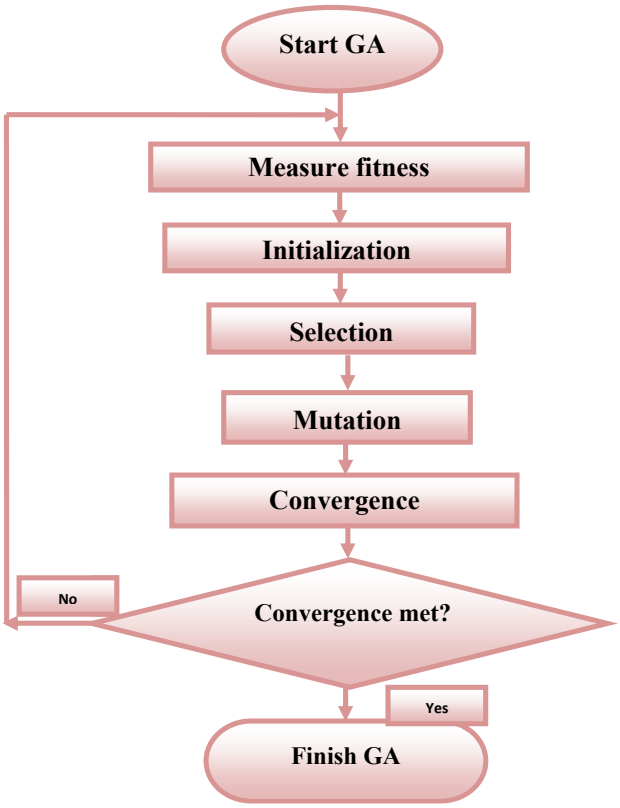

Figure 4. Flowchart of GA.

shown in Figure 4 and the parameters associated with the implementation of these procedures done in software are shown in Table 3.

2.8. Statistical comparison of the models

The statistical methods used to ascertain the degree at which the models represent the experimental data were done by determining R^2, Adj. R^2, MSE, RMSE, SEP and AAD. These were ascertained using Eqs. (6), (7), (8), (9), (10), and (11) as applied by Esonye et al., (2019c).

$$R^2 = 1 - \frac{\sum_{i=1}^{n}\left(Y_{ip} - Y_{ie}\right)^2}{\sum_{i=1}^{n}\left(Y_{ip} - Y_{e}\right)^2} \tag{6}$$

$$\text{Adj. } R^2 = 1 - \left[\left(1 - R^2\right) \times \frac{n-1}{n-K-1}\right] \tag{7}$$

$$MSE = \sum_{i=1}^{n} \frac{\left(Y_{a,i} - Y_{p,i}\right)^2}{n} \tag{8}$$

Table 3. Set genetic algorithm.

Functions mutations	Heuristic
Type of population	Bit string
Crossover	1/intermediate
Selection function	Stochastic uniform
Inheritance of	0.8
Generation	15–50
Mutation rate	0.01/uniform
Population size	100^{th}
Creation function	Uniform

$$RMSE = \sqrt{\frac{\sum_{i=1}^{n}\left(Y_{ie} - Y_{ip}\right)^2}{n}} \tag{9}$$

$$SEP = \frac{RMSE}{Y_e} \times 100 \tag{10}$$

$$AAD = \frac{100}{n}\sum_{i=1}^{n}\frac{\left|Y_{ip} - Y_{ie}\right|}{\left|Y_{ie}\right|} \tag{11}$$

In this study, Y_{ie}, Y_{ip}, Y_e and n represents the experimental values, predicted data, mean value of experimental vales and number of experimental runs respectively.

3. Results and discussion

3.1. RSM optimization of DESO oil extraction

Box Behnken design of experiment was applied to develop a relationship between the factors affecting the DESO yield. The responses obtained from different experimental runs carried out by combination of three variables are presented in Table 4. The three experimental variables interaction gave a total of 17 experimental runs which consists of 12 independent runs and five similar runs. The range of values of the actual, RSM predicted and ANN predicted oil yields respectively were 43.0–51.21, 40.47–52.96 and 42.50–52.80 for n-hexane, 29.04–40.14, 31.17–36.40 and 29.74–39.61 for ethanol and 28.50–31.60, 24.75–30.26 and 27.51–31.42% for M/C.

3.1.1. Regression analysis, ANOVA and model equations

The general approach to fit empirical model with collected response variable data is regressional analysis and responses obtained in Table 4 were correlated with the three independent variables using the polynomial equation in Eq. (2). Summaries of the analysis of variance are tabulated in Table 5. Based on the low p-values ($\leq$0.05) and larger t-values from the results of the ANOVA as contained in Table 6, the following model terms: X_1, X_3, X_1^2, X_1X_2 and X_1X_3 have significant effect on n-hexane response, X_2, X_3, $X_2^2, X_3^2$and X_1X_2 terms had significant effect on ethanol response while M/C response was significantly affected by X_1, $X_3 X_1X_3, X_1^2$, and X_2^2. X_3 which represents the ratio of solute/solvent and was found to have significant effect on the response variables. The significance of this variable was found to decrease from hexane to ethanol and to methanol/chloroform. The reason could be due to the difference in flammability, diffusion rate and miscibility attributes of the solvents that could have affected the rate of solute distribution in these solvents. However, the values of the correlation coefficients ranged $0.95 < R^2 < 1.0$ and this implies that more than 95% of the variations in the responses can be explained by the regression model as a mark of good relationship between the RSM predictions and the experimental values. From the regression analysis, the most fitted models based on the coded values and significance of factors is shown in Eqs. (12), (13), and (14).

$$Y_{n-hexane}\ (wt\%) = 184.44 + 0.3236x_1 - 1.9732x_2 - 1256.4x_3 - 0.000205x_1x_2 - 0.1033x_1x_3 + 15.639\ x_2x_3 - 0.00023x_1^2 - 0.008062x_2^2 + 937.88x_3^2 \tag{12}$$

$$Y_{ethanol}\ (wt\%) = -133.05 + 0.1440x_1 - 4.7335x_2 - 154.07x_3 - 0.0038x_1x_2 - 0.1614x_1x_3 + 2.1449\ x_2x_3 - 0.0001x_1^2 - 0.0370x_2^2 + 401.92x_3^2 \tag{13}$$

$$\mathbf{Y_{M/C}(wt\%) = 12.1577 + 0.1178x_1 - 0.5853 - 153.46x_3 - 0.0015x_1x_2 - 0.1207x_1x_3 + 2.997\ x_2x_3 - 0.00001x_1^2 - 0.0075x_2^2 + 86.13x_3^2} \tag{14}$$

Table 4. Coded factors with actual values and predicted values of RSM and ANN.

Run	Variables			Responses (wt%)								
	Factor1 X_1 (μm)	Factor 2 X_2 (min)	Factor 3 X_3 (g/ml)	n-hexane			Ethanol			M/C		
				Actual	RSM	ANN	Actual	RSM	ANN	Actual	RSM	ANN
1	-1	-1	0	47.1000	46.3880	48.0153	30.1500	34.6958	29.7474	28.9200	26.8560	28.4279
2	1	-1	0	51.2100	52.9619	49.2408	35.2500	31.6613	34.3150	31.6100	30.2590	31.4179
3	-1	1	0	45.5000	43.7912	46.4153	37.1900	36.7109	37.2522	30.0400	25.9250	29.8364
4	1	1	0	43.0000	42.2189	42.5018	29.0400	32.2919	31.5097	27.4400	24.7510	27.5176
5	-1	0	-1	45.5000	41.5155	44.9521	37.1900	36.0069	37.2409	30.0400	26.0273	27.3925
6	1	0	-1	45.5000	40.9589	45.5438	37.1900	33.7683	35.9994	30.0400	25.1717	30.0811
7	-1	0	1	48.1000	46.8072	48.5494	30.8100	31.7926	30.6989	28.5000	27.1479	28.1683
8	1	0	1	50.1000	47.9723	50.7157	34.6200	32.2447	33.8315	30.9400	28.3045	30.9200
9	0	-1	-1	44.2400	40.4764	45.4517	33.6400	33.2413	34.8179	29.7400	25.9712	30.0571
10	0	1	-1	48.1000	44.5361	48.1343	30.8100	31.1728	30.8408	28.5000	24.9999	27.7775
11	0	-1	1	56.3000	43.0237	52.8015	40.1400	37.0055	34.0959	33.7800	28.6575	32.5643
12	0	1	0	43.3000	45.3538	41.0337	29.0400	33.3283	39.6102	27.4400	25.4379	26.9582
13	0	0	0	47.2100	48.3135	48.5474	30.1100	36.4062	30.7044	28.0000	26.8870	29.0706
14	0	0	0	48.5000	48.3135	48.5474	30.9200	36.4062	30.7044	28.9700	26.8870	29.0706
15	0	0	0	50.2100	48.3135	48.5474	34.7700	36.4062	30.7044	31.5600	26.8870	29.0706
16	0	0	0	49.6100	48.3135	48.5474	32.4500	36.4062	30.7044	28.8400	26.8870	29.0706
17	0	0	0	45.5000	48.3135	48.5474	33.1900	36.4062	30.7044	30.0400	26.8870	29.0706

Table 5. Results of the ANOVA.

Responses	Source	Coefficients	t-statistics	P-val Remarks	SSE	MSE	Df
N-hexane oil yield	Model	a_0	-3.0742	0.0120 *Significant*	25.1889	5.5765	9
	X_1	a_1	2.6527	0.0278 *Significant*	2.3404	2.3404	1
	X_2	a_2	2.2809	0.0453 *Significant*	0.5851	0.5851	1
	X_3	a_3	3.0800	0.0133 *Significant*	0.0245	0.0245	1
	X_1X_1	a_4	0.5625	0.6262	0.0173	0.0173	1
	X_2X_2	a_5	-2.8317	0.0183 *Significant*	0.0007	0.0007	1
	X_3X_3	a_6	-1.4425	0.1798	0.0002	0.0002	1
	X_1X_2	a_7	-2.3750	0.0350 *Significant*	0.0389	0.0389	1
	X_1X_3	a_8	-2.1824	0.0383 *Significant*	0.0024	0.0024	1
	X_2X_3	a_9	-1.9652	0.0919	0.0001	0.0001	1
Ethanol oil yield	Model	a_0	2.7750	0.0261 *Significant*	38.6348	0.1816	9
	X_1	a_1	0.8505	0.4668	0.0762	0.0762	1
	X_2	a_2	-2.8175	0.0430 *Significant*	0.0191	0.0191	1
	X_3	a_3	3.1015	0.0153 Significant	0.0008	0.0008	1
	X_1X_1	a_4	0.8036	0.4458	0.0006	0.0006	1
	X_2X_2	a_5	2.5700	0.0420 *Significant*	0.0001	0.0001	1
	X_3X_3	a_6	-2.0808	0.0463 *Significant*	0.0001	0.0001	1
	X_1X_2	a_7	-2.0080	0.0290 *Significant*	0.0013	0.0013	1
	X_1X_3	a_8	0.7808	0.4553	0.0001	0.0001	1
	X_2X_3	a_9	-1.0518	0.3176	0.0001	0.0001	1
M/C oil yield	Model	a_0	2.9558	0.0171 *Significant*	19.2649	0.1405	9
	X_1	a_1	2.8775	0.0139 *Significant*	0.0590	0.0590	1
	X_2	a_2	1.2045	0.2561	0.0147	0.0147	1
	X_3	a_3	2.8214	0.0181 *Significant*	0.0006	0.0006	1
	X_1X_1	a_4	2.8410	0.0195 *Significant*	0.0004	0.0004	1
	X_2X_2	a_5	-2.1473	0.0574	0.0001	0.0001	1
	X_3X_3	a_6	0.8634	0.4134	0.0001	0.0001	1
	X_1X_2	a_7	-1.8883	0.0899	0.0010	0.0010	1
	X_1X_3	a_8	-2.8178	0.0216 *Significant*	0.0001	0.0001	1
	X_2X_3	a_9	-2.7266	0.0151 *Significant*	0.0001	0.0001	1

3.1.2. *Combined effects of operating conditions*

The extraction process of *Dyacrodes edulis* seed oil using different solvents (n-hexane, ethanol and a mixture of methanol and chloroform) were analyzed based on the various solutions obtained at possible reacting conditions from the model predictive equations. The flexibility of RSM in navigating the design space makes it very appropriate. The

Table 6. Comparison of statistical indices of RSM and ANN models.

Parameters	N-hexane		Ethanol		M/C	
	RSM	ANN	RSM	ANN	RSM	ANN
R^2	0.89	0.93	0.87	0.91	0.86	0.89
R	0.94	0.96	0.93	0.91	0.92	0.94
Adj. R^2	0.76	0.841	0.74	0.86	0.71	0.76
MSE	2.729	2.824	2.041	1.750	1.580	1.672
RMSE	4.450	4.543	3.352	3.299	3.224	3.033
SEP	160.595	55.710	188.987	186.003	189.515	60.700
AAD	2.5561	2.1888	2.7525	4.4027	2.5763	2.8479

interactions between only two factors were considered at any particular instance while setting the other variable at itsr mean coded values of zero (0). The interactive effects of adjusting the process variables within the design space were monitored using the 3D surface plots and every significant interactive affects. The analysis and optimization exercises were completed using the MATLAB 8.5 version and the graphical solutions are presented in Figures 5, 6, and 7 as response contour plots. The simultaneous effect of particle size and extraction time on the DESO yield from the three solvents showed similar trend (Figure 5). It was observed that before 400μm, oil yield decreased while oil yield increased with increase in extraction time at all particle sizes. Basically, smaller particle size is expected to give more yield due to effective surface area, but within the range of 300–500μm studied, it was observed that below 400μm gave lesser yield which could be due to agglomeration of the particles that reduced the surface area (Musa et al., 2015). However, above 450μm, the oil yield decreased probably due to reduced available surface area for the solute and solvent contact. The effect of particle size and solute/solvent ratio on the oil yield is presented in Figure 6. The effect of particle size was found to be similar to that observed in Figure 4. The maximum oil yield was observed at higher particle sizes and 0.20 solute/solvent ratios were found to give the lowest oil yield. It was observed that to achieve higher oil DESO yield while using any of the selected solvents, solute/solvent ratio below 0.2 and particle size between 400 and 450um are optimum. This result is supported by previous findings (Anwar et al., 2005; Borchani et al., 2010). The interactive effect of solute/solvent ratio and extraction time on oil yield is shown in Figure 7. Maximum oil yield was obtained at 60min and 0.24 solute/solvent ratios. Also, lower solute/solvent ratio (which implies more solvent) and lower extraction time around 45min gave higher oil yield. It implies that to achieve high oil yield from DESO using the selected solvents requires high amount of solvents and low contact time or less extraction time and solvent.

3.2. ANN modeling of DESO oil extraction

Ascertaining the required number of neurons in the hidden layer is very important. Basically, a trial and error approach was used as the technique to achieve minimum deviations of the predicted responses from the practical values. The best architecture generated by MATLAB 8.5, 2015 version software is depicted in Figure 8. It has three layers, comprising of three (3) input neurons, four (4) hidden neurons and one (1) output neuron. The three (3) input neurons represent the extraction time, solute/solvent ratio and solute particles sized while the output neuron represents the DESO yield. Many training runs were carried out in search of the minimum weights in the error propagation framework. N-hexane, ethanol and M/C solvents extractions had 13,17 and 15 iterations respectively prior to achieving minimum possible weight during the training to achieve the final selected architecture. For three (3) different solvent types studied, the network was trained using 11 experimental data, and validated using three (3) experimental data. Also, three (3) remaining experimental data were used for testing the network. Figure 9a–c shows the plots of validation against target for linear fit models of n-hexane (Y = 0.65* Target + 16), ethanol (Y = 1.3* Target+ 7.5) and M/C (Y = 1.2* Target + 4.5). The ANN model values were predicted using the above equations. The mean square error (MSE) of the network and corresponding coefficient of correlation (R) are presented in Figure 10a for n-hexane, Figure 10b for ethanol and Figure 10c for M/C.

3.3. 3 RSM and ANN model comparison

Table 6 contains the comparison of the results of the statistical analysis of the RSM and ANN models using standard statistical indices. The MSE, RMSE, SEP and AAD as well as the R^2 and adjusted R^2 of the models were determined. The results clearly indicate that both models were highly efficient in correlating with the practical values. A minimum value of 0.8 for R shows good correlation between predicted and actual (practical) values (Betiku et al., 2018). In this study, all the R were in above 0.91, R^2 values were in the range of $0.86 < R^2 < 0.94$ while the values of adj. R^2 values were in the range of $0.76 <$ adj. $R^2 < 0.87$. These results show that the models were statistically significant. The results of the error indices were comparatively low for both RSM and ANN models. However, the RSM model was the less efficient while the ANN model was fairly better in all the three solvents types applied for DESO extraction. Therefore, ANN showed better prediction capability, fitting ability and generalization capacity than RSM. This could be due to its approximation ability through nonlinearity of the system while RSM belongs to only a second-order polynomial. However, the challenge of using ANN technique is in its sensitivity to the number of hidden neurons and overtraining (Morteza et al., 2018).

3.4. RSM and ANN - GA DESO extraction optimized conditions and experimental validation

The results of the optimized conditions using the numerical solution capability of the RSM and ANN-GA interface techniques are presented in Table 7. N-hexane recorded highest oil yield even at almost the same conditions of extraction. Therefore, ANN model was coupled with global optimization method: genetic algorithm (GA). Genetic algorithm was applied to obtain the best conditions for the process variables combinations for maximum oil yield using the ANN developed models. The fitness values increased from G1 to G10 and remained constant afterwards (Figure 11) and this shows that there were no gene mutations that could affect the response (DESO yield). The RSM optimal predicted oil yields were 45.21%, 38.61% and 30.87% while experimental values were 46.01%, 40.71% and 32.45% for n-hexane, ethanol and M/C respectively. The RSM optimum conditions were particle sizes of 450.67, 451.19 and 450.22μm, extraction times of 55.57, 55.16 and 56.11min and solute/solvent ratios of 0.19, 0.16 and 0.18 g/ml for n-hexane, ethanol and M/C respectively. The ANN-GA optimized conditions showed 5.14, 5.81 and 2.12 % higher DESO yields at 1.10, 0.26 and 0.65% smaller particle sizes, 5.47, 0.30

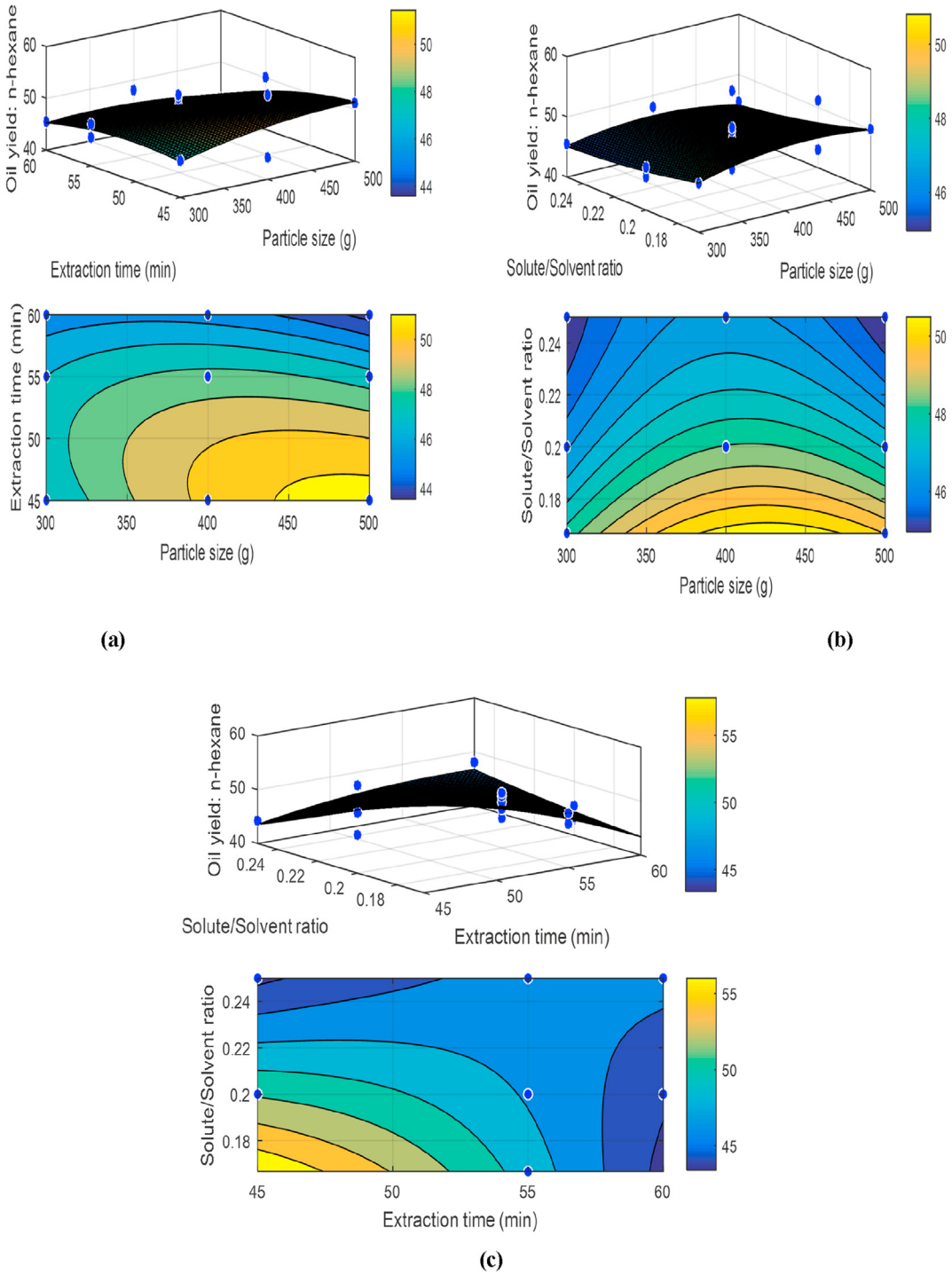

Figure 5. 3D response surface plot of the effects of the variables on DESO yield using n-hexane: (a)-particle size versus extraction time; (b)-particle size versus solute/solvent ratio and (c)-extraction time versus solute/solvent ratio.

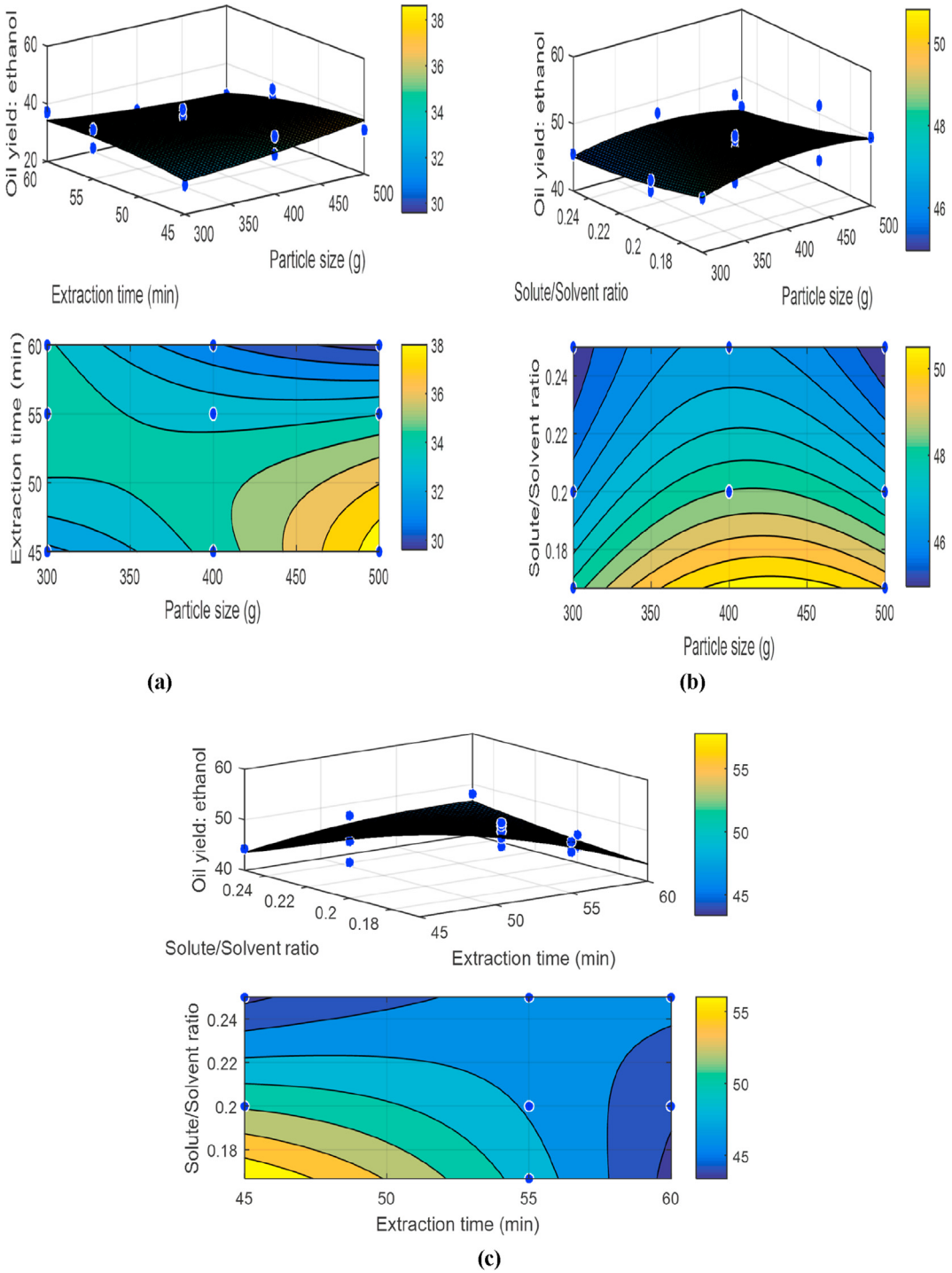

Figure 6. 3D response surface plot of the effects of the variables on DESO yield using ethanol: (a)-particle size versus extraction time; (b)-particle size versus solute/solvent ratio and (c)-extraction time versus solute/solvent ratio.

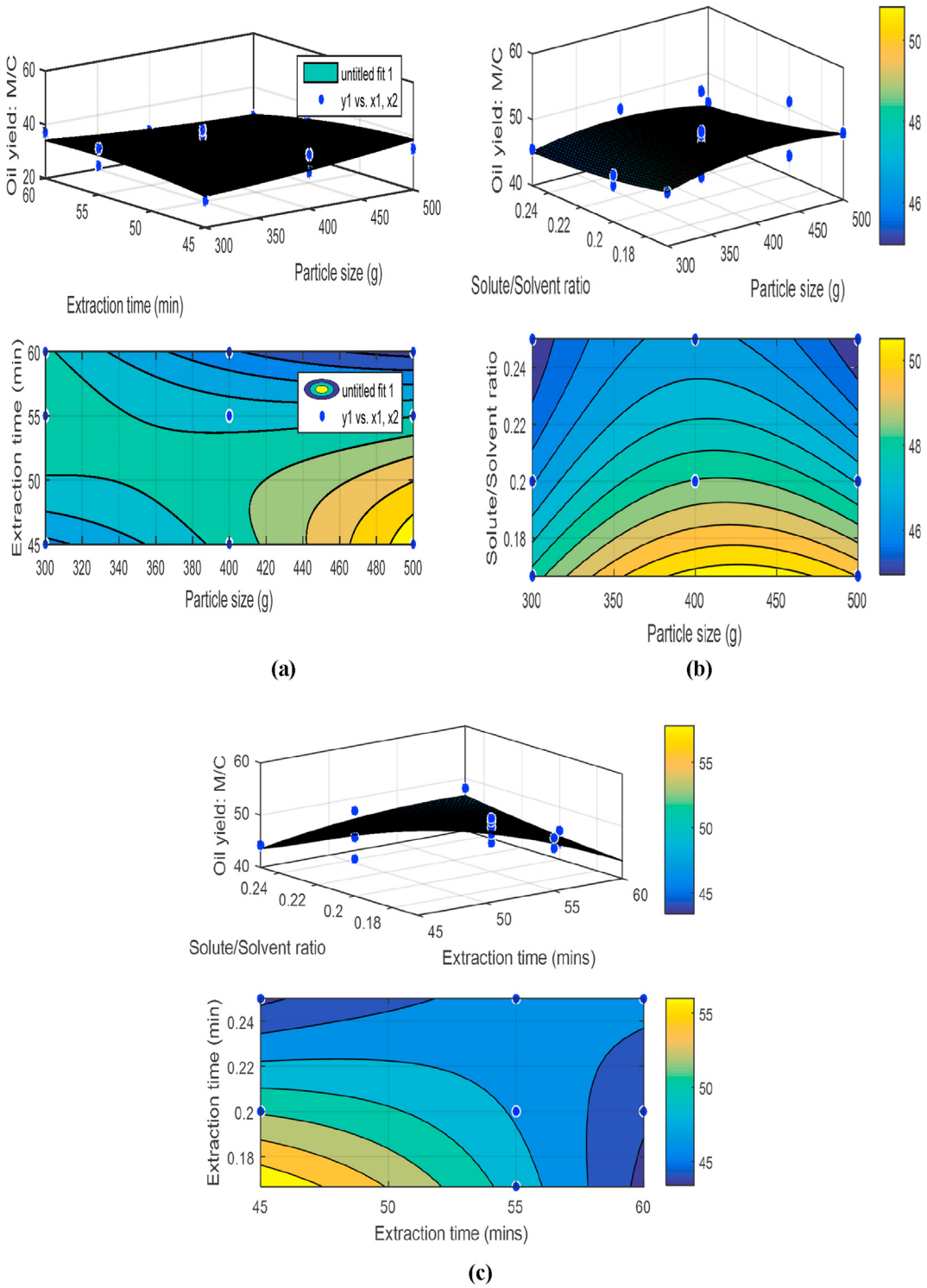

Figure 7. 3D response surface plot of the effects of the variables on DESO yield using M/C: (a)-particle size versus extraction time; (b)-particle size versus solute/solvent ratio and (c)-extraction time versus solute/solvent ratio.

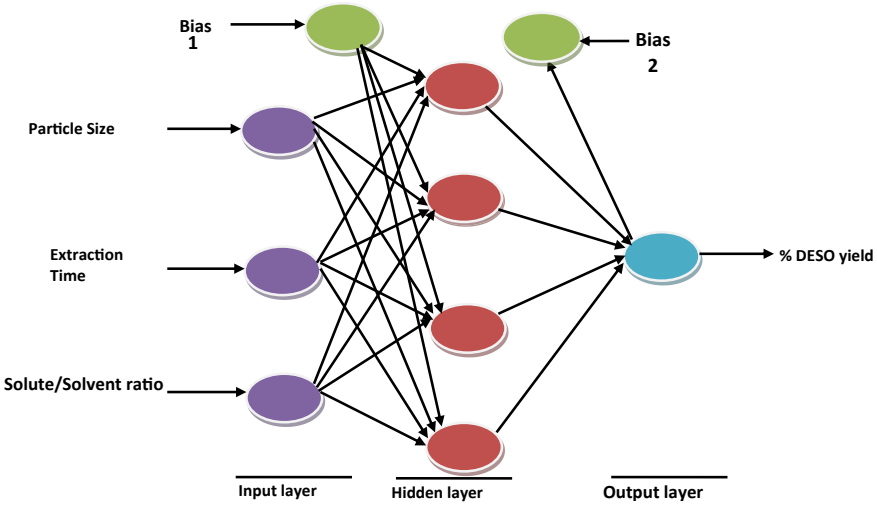

Figure 8. 3-4-1 ANN model architecture topology for the oil extraction.

and 0.62 % faster rates, and 24, 11.11 and 10% more solute requirements for n-hexane, ethanol and M/C solvents respectively. Similar results showing the supremacy of ANN-GA over RSM optimization tool has been reported previously (Okeleye and Betiku, 2019). The maximum experimentally validated oil yield of 48.89% was obtained using n-hexane and ANN-GA conditions. It is higher than 42.12% and 33.02% obtained using ethanol and M/C respectively. This is in agreement with previous authors reports which was due to the fact that n-hexane possesses superior attributes of simple recovery, low latent heat of vaporization (330 kJ/kg), narrow range of boiling point (63–69 °C), high solubility and non-polar nature (Mwaura et al., 2020). More so, the highest oil yield of 48.89% obtained in this study is less than 56.30 and 57.97% previously reported on the same feedstock (Esonye et al., 2019c; Ofoefule et al., 2019). The reason is that these higher oil yields were conducted at different higher extraction time of 24 h against the maximum of 1h used in this study. This shows that the optimum time in this study is more economical. However, considering environmental factors, cost of labour and other related governmental policies, any of the solvents could be applied for DESO extraction.

3.5. DESO quality characteristics

3.5.1. DESO functional groups

Table 8 contains the main functional groups present in DESO at the optimum conditions of n-hexane extraction. The absorption peaks appearing at 760.18cm^{-1} represents the bending vibrations of alkenes and overlapping of rocking vibrations of methylene for both samples. The other ones at 895.28 and 930.02cm^{-1} represents the bending vibrations of C–H and = C–H functional groups for alkanes and alkenes unsaturated class respectively. The 1165.48cm^{-1} stretching vibrations of DESO spectra represents the single bond carbonyl functional groups (C–O). The characteristics peaks found at 1223.38cm^{-1} for DESO indicates the bending vibrations of C–O–C. The band regions of 1346.90–1578.50cm^{-1} in the DESO spectrum can be asserted to the bending vibration of –CH_2 methyl groups in the fatty acid (Gunstone, 2004). The 1721.32cm^{-1} in the DESO is attributed to C–O groups with the stretching mode of vibration. These indicate the presence of carbonyl functional groups that appear as R_1–C(OR)–O in the vegetable oil. The peaks at the regions of 3134.08–3265.3cm^{-1} in the DESO spectra is attributed to the stretching vibrations of = C–H alkene groups. The peak 3790.20cm^{-1}for DESO with stretching mode of vibration is ascribed to the presence of O–H groups (Shut et al., 2010). They are single bonded at high energy frequency and attributed to undesirable water present in the samples. The presence of carbon to carbon (C=C) can cause the oil samples to remain in liquid state but may be liable to possible oxidation during long term storage. However, all the observed absorptions corresponding to C=O stretches show that the seed oil is biodegradable.

3.5.2. DESO fatty acid composition

From Table 9, oleic; α-linoleic, stearic, linolenic, palmitic and behenic acids were the most prevalent fatty acid found in DESO. It was observed that the percentage abundance of the fatty acids follows the following order: monounsaturated > saturated > polyunsaturated fatty acids. DESO would possess high melting pointv due its high saturated fatty acid content and this would make it to be useful for many industrial applications such as surfactants and detergents. Also the amount of fatty acid present in DESO is found to compare well with others in oleic family (Esonye et al., 2019b). It will therefore found useful applications in nutrition and as non-drying oil upon slight modifications (Uzoh and Onukwuli, 2016; Obiegu-Nwosu et al., 2020). The seed oil's high monounsaturated fatty acid content (57.84%) supports its previously reported high potential for biodiesel production (Esonye et al., 2019c).

3.5.3. DESO physico-chemical properties

Table 10 contains the physico–chemical characteristics of the seed oil extracted from *Dyacrodes edulis* seed using n-hexane. The properties compare favourably with previous reports (Esonye et al., 2019a). Although n-hexane had the highest oil yield followed by ethanol and least by M/C, the other properties of the oil showed insignificant variations in values. It implies that solvent type has little impact on the physical qualities of the refined oil. These results show that DESO compared favourably with other seed oils applied for edible and industrial purposes (Esonye et al., 2019a). Extensive reports on physico-chemical properties of DESO have been previously presented (Esonye et al., 2019a; Ofoefule et al., 2019) and the results are similar to what is obtained in this study. Although the seed samples were collected from different locations within the same geographical part of Nigeria, the results compared well with slight deviations which could be due to differences in variety and processing methods. The flash points were above 149 (°C), this implies that the extracted oil would found useful application as a biodiesel since it is within the ASTM D 6751 limits of 100–170 and would not be prone to fire disaster during handling. However, the acid value 8.02 (mgKOH/g) appears higher than 3.28 mgKOH/g) (Ofoefule et al., 2019) and lower than 12.33 mgKOH/g (Esonye et al., 2019a) from same feedstock and far less than 47.12 and 51.4 mgKOH/g reported on paw-paw and orange seeds (Esonye et al., 2019a). It implies that the oil requires esterification as pretreatment before it could

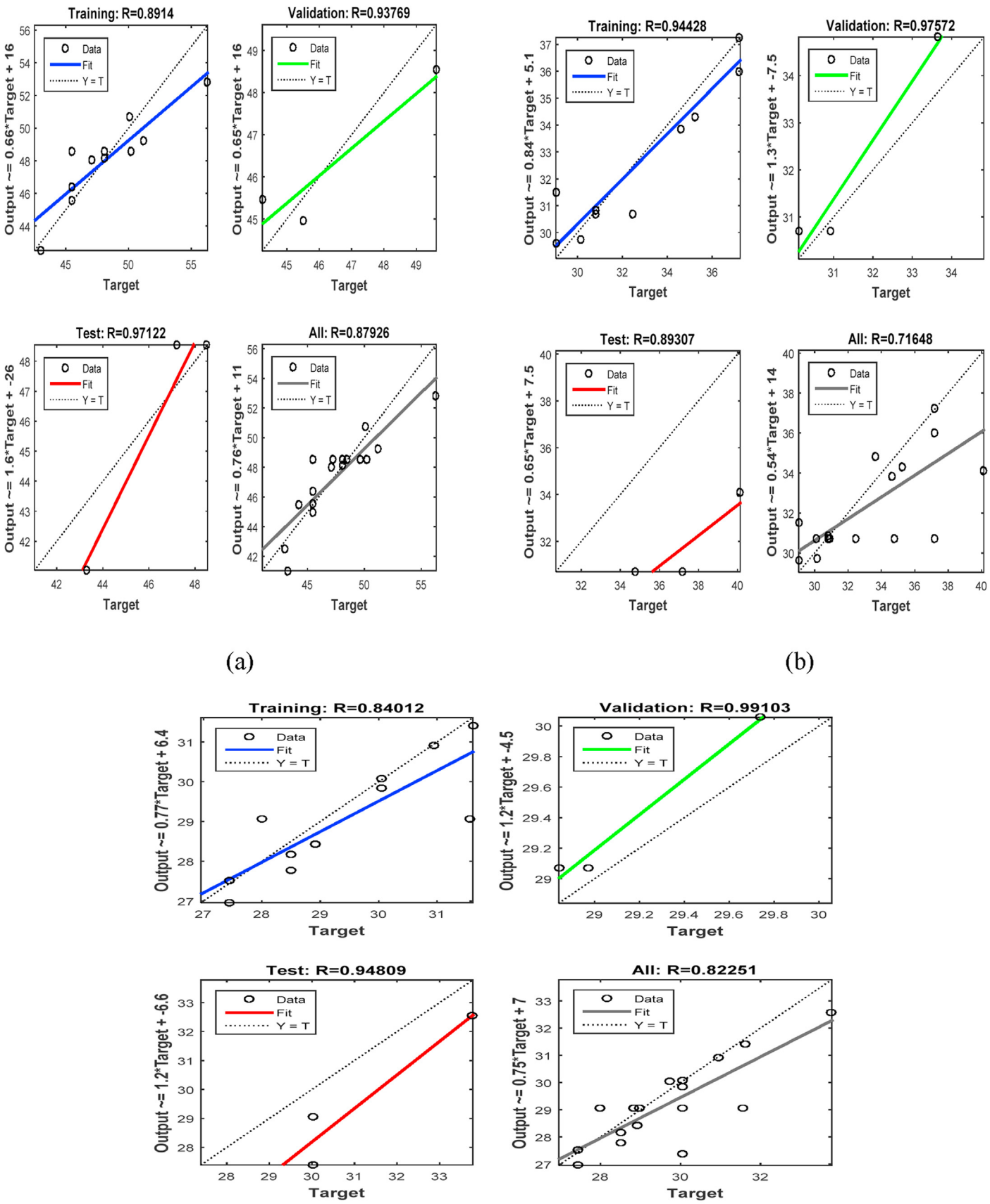

Figure 9. ANN regression values for training, test, validation and overall model for: (a) n-hexane, (b). ethanol and (c). M/C extractions.

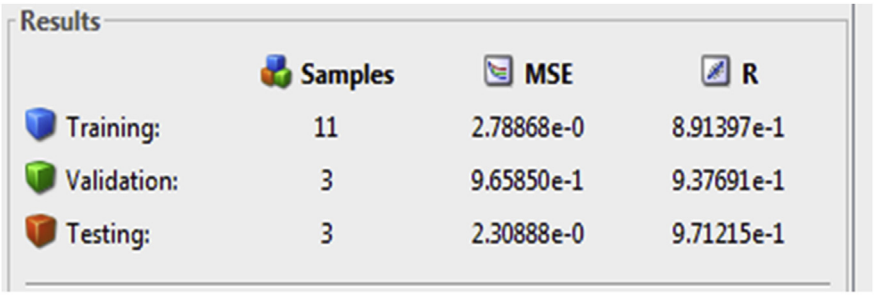

(a)

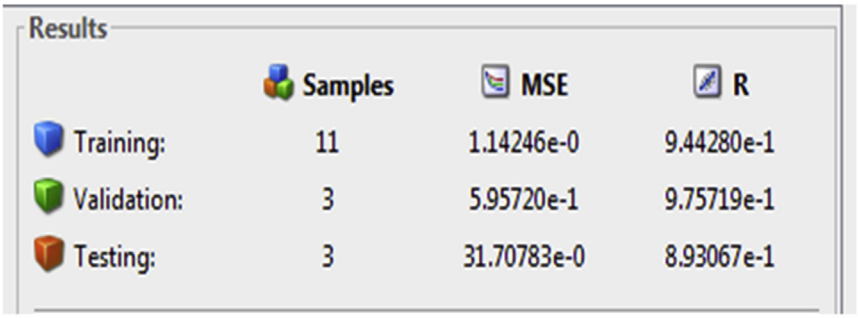

(b)

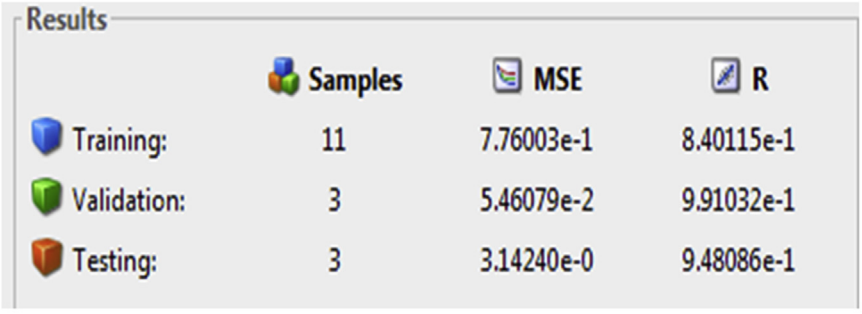

(c)

Figure 10. MSE and R for training, validation and testing of DESO extraction:(a). n-hexane, (b). Ethanol and (c). M/C.

Table 7. Optimized conditions and experimental validation.

Solvent type: Optimization tool	Optimized DESO yield (wt %)	Experimental DESO yield (wt %)	Optimum conditions		
			Particle size (μg)	Extraction time (min)	Solute/solvent (g/ml)
N-hexane: RSM	45.21	46.01	450.67	55.57	0.19
ANN-GA	47.66	48.89	445.71	52.53	0.25
Ethanol: RSM	38.61	40.71	451.19	55.16	0.16
ANN-GA	38.99	42.12	450.02	55.00	0.18
M/C: RSM	30.87	32.45	450.22	56.11	0.18
ANN-GA	31.54	33.02	447.34	55.76	0.20

undergo transesterification process for biodiesel production. Also, the specific gravity of 0.888 is within the 860–900 limits for EN 14214 for biodiesel which implies that its application in diesel engines would promote efficient combustions conditions for air-fuel ratio. The moisture content results would not have any adverse effect on the seed oxidation stability and shelf life in case of long term storage. The low iodine value indicates less unsaturation and comparatively less prone to oxidation instability and glyceride polymerization that normally leads to formation of deposits. The peroxide and iodine values indicate that the oil can be modified to bio based resins for plastic and paint industries (Obiegu-Nwosu et al., 2020).

4. Conclusion

MATLAB 8.5, 2015 version software was used to investigate the optimum conditions for optimal seed oil extraction from *Dyacrodes edulis* using different solvents (n-hexane, ethanol and mixture of methanol and chloroform) by applying artificial neural network-genetic algorithm (ANN-GA) and response surface methodology (RSM). N-hexane gave the highest oil yield of 45.21% and experimental validation value of 46.01% at particle size of 450.75μg, extraction time of 55.57min and solute/solvent ratio of 0.19 using Box-behnken experimental design of response surface methodology (RSM) based on

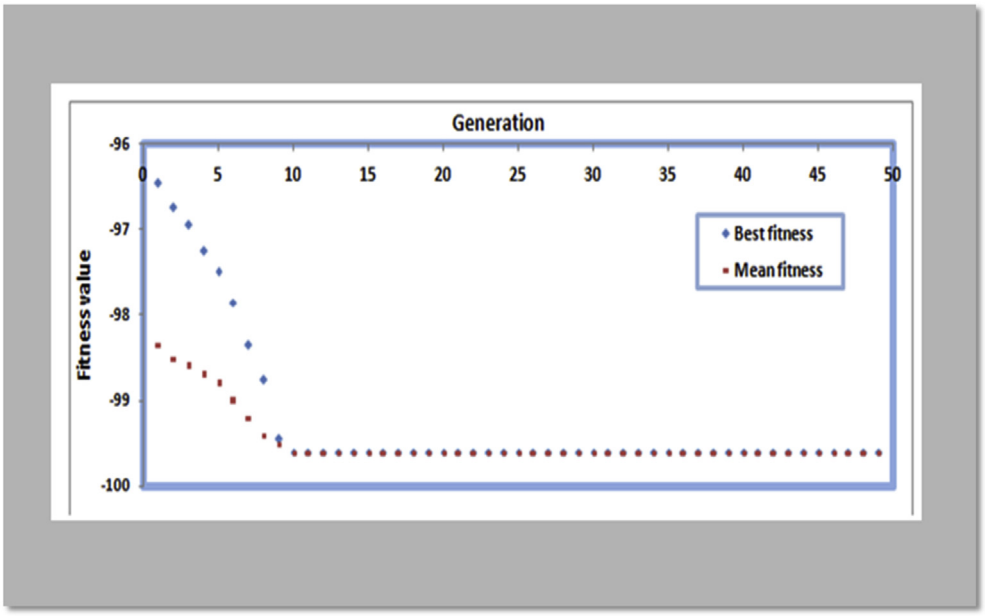

Figure 11. Fitness value versus generation using ANN-GA.

Table 8. FT-IR main characteristic band positions for DESO using n-hexane.

Wave number (cm^{-1})	Type of vibration	Functional group
760.18	Bending	C–H
895.28	Bending	C–H
1165.48	Stretching	C–O
1223.38	Bending	C–CO–O
1346.90	Bending	CH_2
1439.54	Bending	CH_2
1578.50	Bending	CH_2
1659.56	Bending	C=C
1721.32	Stretching	C=O
3134.08–3265.32	Stretching	= CH,C=C
3790.28	Stretching	O–H

Table 9. The major fatty acid compositions of DESO extracted using n-hexane.

Sn	Fatty acid	Systematic name	Formula	Structure	Amount (%)
1	Palmitic	Hexadecanoic	$C_{16}H_{32}O_2$	$C_{16:0}$	10.65
2	Oleic	cis-9-octadecenoic	$C_{18}H_{34}O_2$	$C_{18:1}$	53.13
3	α-linolenic	cis,cis,cis-9,12,15-octadactrienoic	$C_{18}H_{30}O_2$	$C_{18:3}$	3.40
4	Stearic	octadecanoic	$C_{18}H_{36}O_2$	$C_{18:0}$	12.54
5	Gadoliec	cis-9-eicosenoic	$C_{18}H_{32}O_2$	$C_{20:1}$	4.71
6	Behenic	docosanoic	$C_{22}H_{44}O_2$	$C_{22:0}$	3.18
7	Others	-	-	-	12.39
	SFA				26.37
	MUFA				57.84
	PUFA				3.40

SFA – Saturated fatty acid, MUFA – Monounsaturated fatty acids, PUFA- Polyunsaturated fatty acid.

quadratic model. The ANN-GA gave 5.14, 5.81 and 2.12 % higher DESO yields at 1.10, 0.26 and 0.65% smaller particle sizes, 5.47, 0.30 and 0.62 % faster rates and 24, 11.11 and 10% more solute requirements, for n-hexane, ethanol and M/C solvents respectively. ANN with a multilayer neural network model of 3 input neurons, four (4) hidden neurons and one (1) output neuron showed higher supremacy than RSM based on its higher values of R^2 and lower error indices. ANN showed better prediction capability, fitting ability and data generalization capacity than RSM. Also, ANN-coupled with genetic algorithm gave better optimal route than the numerical optimization tool of RSM. The quality of the oils obtained at the optimum conditions was satisfactory for many commercial purposes.

Table 10. The physico-chemical properties of DESO.

S/N	Properties	Results		
		Ethanol	n-hexane	M/C
1.	Average oil yield (%)	42.12 (3.34)	48.89 (4.15)	33.02 (3.76)
2.	Specific gravity	0.8885 (0.006)	0.8884 (0.007)	0.88890 (0.008)
3.	Moisture content (%)	0.50 (0.040)	0.48 (0.055)	0.55 (0.030)
4.	Iodine value (gI^2/g)	36.15 (4.12)	36.05 (5.58)	36.50 (3.77)
5.	Free fatty acid on oleic (mgKOH/g)	4.01 (0.30)	4.01 (0.35)	4.01 (0.40)
6.	Peroxide value (meq/kg)	1.855 (0.03)	1.876 (0.02)	1.864 (0.03)
7.	Saponification value (mg KOH/g oil)	249.04 (3.50)	250.67 (2.50)	250.02 (3.30)
8.	Viscosity (Cp)	5.94 (0.29)	6.04 (0.25)	5.80 (0.30)
9.	Acid value (mgKOH/g)	8.02 (0.25)	8.02 (0.20)	8.02 (0.30)
10.	Flash point (°C)	149.05 (2.26)	149.61 (2.01)	149.22 (2.52)

Values are means of triplicate determination and standard deviation (SD) are given in parenthesis.

Declarations

Author contribution statement

Esonye, C & Onukwuli, O. D.: Conceived and designed the experiments; Performed the experiments; Analyzed and interpreted the data; Wrote the paper.

Anadebe, V.C & Ezeugo, J.N.O.: Performed the experiments; Analyzed and interpreted the data; Contributed reagents, materials, analysis tools or data.

Ogbodo N. J: Performed the experiments; Analyzed and interpreted the data; Wrote the paper.

Funding statement

This research did not receive any specific grant from funding agencies in the public, commercial, or not-for-profit sectors.

Data availability statement

Data will be made available on request.

Declaration of interests statement

The authors declare no conflict of interest.

Additional information

No additional information is available for this paper.

Acknowledgements

The authors are grateful to the National Centre for Energy Research and Development (NCERD), University of Nigeria Nsukka and National Research Institute for Chemical Technology (NARICT), Ahmmadu Bello University (ABU), Zaria, Nigeria for the availability of the laboratory facilities, apparatus and analytical equipment.

References

Achten, W.M.J., Verchit, L., Mathisjs Franken, Y.J., Singh, E., Arts, V.P., Muijs, R.B., 2008. Jatropha biodiesel production and use. Biomass Bionergy 32 (12), 1063–1084.

Adebayo, S.E., Orheuba, B.A., Adeoye, P.A., Musa, J.J., Fase, O.J., 2012. Solvent extraction and characterization of oil from African star apple (*Chrysophyllum albidium*) seeds. Acad. Res. Int. Nat. Appl. 3 (2), 178–183.

Adepoju, T.F., Rasheed, B., Olatunji, O.M., Ibeh, M.A., Ademiluyi, F.T., Olatunbosun, B.E., 2018. Modeling and optimization of lucky nut biodiesel production from lucky nut seed by pearl spar catalysed transesterification. Heliyon 4, e00798.

Aiwize, E.A., Achebo, J.I., 2012. Liquid Soap Production with blends of Rubber Seed oil (RSO) and Palm kernel oil (PKO) with locally sourced caustic potash (Kolt). Nigerian J.Tech. 31 (10), 63–67.

Anwar, F., Ashraf, M., Bhanger, M.I., 2005. Interprovenance variation in the composition of moringa oleifera oil seed from Pakistan. J. Am. Oil Chem. Soc. 82, 45–51.

AOAC, 2000. Official Methods of Analysis, thirteenth ed. Association of Official Analytical Chemists, Washington, DC.

ASTM D2500- Standard Test Method for Testing of Flash point from the SAI Global.

Atabani, A.E., Silitonga, A.S., Irfan, A.B., Mahlia, T.M.I., Masjuki, H.H., Mekhilef, S., 2012. A comprehensive review on biodiesel as an alternative energy resource and its characteristics. Renew. Sustain. Energy Rev. 16, 2070–2093.

Bello, E.I., Fade-Aluko, A.O., Anjorin, S.A., Mogaji, T.S., 2011. Nut Dika nut (*Irvingia gabonensis*) oil biodiesel as alternative fuel for diesel engines. J. Petro. Technol. Alternative Fuels 2 (9), 176–180.

Betiku, E., Adepoju, T.F., 2013. Methanolysis Optimization of Sesame (*Sesamum indicum*) oil to biodiesel and fuel quality characterization. Int. J. Energy Environ. Eng. 4 (9), 1–8.

Betiku, E., Osunleke, A., Odude, V., 2018. Performance evaluation of adaptive neuro-fuzzy inference system, artificial neural network and response surface methodology in modeling biodiesel synthesis from palm kernel oil by transesterification. Biofuels 2018, 1–16.

Borchani, C., Besbes, S., Blecker, C., Attia, H., 2010. Chemical characteristics and oxidation stability of sesame seed, sesame paste and olive oils. J. Agric. Sci. Technol. 12, 585–596.

Castejon, N., Luna, P., Senorans, F.J., 2018. Alternative oil extraction methods from *Echium plantagineum L.* seeds using advanced techniques and green solvents. Food Chem. 244, 75–82.

Chemat, F., Abert Vian, M., Ravi, H.K., Khadhraoui, B., Hilali, S., Perino, S., Tixier, A.S.F., 2019. Review of alternative solvents for green extraction of food and natural products: panorama, principles, applications and prospects. Molecules 24 (16), 3007.

Dash, S.N., Narumanchi, S., Paavola, J., Perttunen, S., Wang, H., Lakkisto, P., Tikkanen, I., Lehtonen, S., 2017. Sept7b is required for the subcellular organization of cardiomyocytes and cardiac function in zebrafish. Am. J. Physiol. Heart Circ. Physiol. 312 (5), H1085–H1095.

Das, A.K., Dewanjee, S., 2018. Optimization of extraction using mathematical models and computation. In: Satyajit, D.S., Lutfun, N. (Eds.), Computational Phytochemistry. Elsevier, pp. 75–106.

Esonye, C., Onukwuli, O.D., Ofoefule, A.U., 2019a. Characterization and oxidation modeling of oils from *prunus amygdalus, dyacrodes edulis* and *chrysophyllum albidium*. Ind. Crop. Prod. 128, 298–307.

Esonye, C., Onukwuli, O.D., Ofoefule, A.U., Ume, C.S., Ogbodo, J.N., 2020. Sea almond as a promising feedstock for green diesel: statistical optimization and power rate law based chemical kinetics of its consecutive irreversible methanolysis. In: Dyzin, K. (Ed.), Prunus. IntechOpen, Netherland, pp. 1–32.

Esonye, C., Onukwuli, O.D., Ofoefule, A.U., Ogah, E.O., 2019b. Multi-input multi-output (MIMO) ANN and Nelder-Mead's simplex based modeling of engine performance and combustion emission characteristics of biodiesel-diesel blend in CI diesel engine. Appl. Therm. Eng. 151, 100–114.

Esonye, C., Onukwuli, O.D., Ofoefule, A.U., 2019c. Chemical Kinetics of a Two-step transesterification of *dyacrodes edulis* seed oil using acid-alkali catalyst. Chem. Eng. Res. Des. 145, 245–257.

Fangrui, M., Hanna, M.A., 1999. Biodiesel production: a review. Bioresour. Technol. 70, 1–15.

Fu, Y.J., Zu, Y.G., Wang, L.L., Zhang, N.J., Liu, W., Li, S.M., Zhang, S., 2008. Determination of fatty acid methyl esters in biodiesel produced from yellow horn oil by RP-LC-RID. Chromatographia 67, 9–14.

Giwa, S., Ogunbona, C., 2014. Sweet almond (*Prunus amygdalus dulcis*) seeds as a potential feedstock for Nigerian biodiesel automotive project. Rev. Ambient Aqua 9 (1), 35–48.

Global Vegetable-Oils-Business-Report, 2018 www.businesssure.com/news/home/20180821005275/en/Global-vegetable-oils.Business-Report- 2018 annual. (Accessed 13 October 2018).

Gunstone, E.D., 2004. Rapeseed and canola oil: production process, properties and uses. JAOCS 33, 132–139.
Igbum, O.G., Leke, L., Ande, S., Okoronkwo, M.U., Nwadinigwe, C.A., 2012. Effects of transesterification variables on the characteristics of the methyl esters obtained from four virgin tropical seed oils in Nigeria. Int. Res. J. Pure Appl. Chem. 2 (4), 230–478.
Keneni, Y.G., Bahiru, L.A., Marchetti, J.M., 2020. Effects of different extraction solvents on oil extracted from jatropha seed and the potential of seed residues as a heat provider. Bioenergy Res.
Kumar, S.J., Kumar, G.V., Dash, A., Scholz, P., Banerjee, R., 2017. Sustainable green solvents and techniques for lipid extraction from microalgae: a review. Algal Res. 21, 138–147.
Lalas, S., Tsakins, J., 2002. Characterization of moringa oleifera seed oil variety "Periyakulum". J. Food Compos. Anal. 15 (1), 65–77.
Morteza, N., Meysam, K., Mohammad, S., Mohammad, D., Mojtaba, K., 2018. Comparison of reponse surface methodology (RSM) and artificial neural networks(ANN) towards efficient optimization of Flexural properties of Gyspum-Bonded fiberboards. CERENE 24 (1).
Musa, U., Isa, A.G., Mohammed, J.A., Mohammed, U.G., Usman, Z., Alharsan, B., 2015. Extraction of *Chrysophyllum albidium* seed oil, optimization and characterization. Chem. Process Eng. Res. 30, 1–8.
Mwaurah, P.W., Kumar, S., Kumar, N., 2020. Novel oil extraction technologies: process conditions, quality parameters, and optimization. Compr. Rev. Food Sci. Food Saf. 19, 3–20.
Nwosu-Obiegu, K., Aguele, F., Cheimenem, L., 2020. Soft computing prediction of oil extraction from Hura crepitan seeds. Kem. Ind. 69, 11–12, 653-658.
Obiegu-Nwosu, K., Aguele, F., Cheimenem, L., 2020. Soft computing Prediction of oil extraction from *Hura crepitan* seeds. Kem. Ind. 69 (11-12), 653–658.
Ochigbo, S.S., Paiko, Y.B., 2011. Effects of solvent blending on the characteristics of oils extracted from the seeds of *Chrysophyllum albidium*. I.J.S.N 2 (2), 352–358.
Ofoefule, A.U., Esonye, C., Onukwuli, O.D., Nwaeze, E., Ume, C.S., 2019. Modeling and optimization of African pear seed oil esterification and transesterification using artificial neural network and response surface methodology comparative analysis. Ind. Crop. Prod. 140, 111707.
Ohale, P.E., Uzoh, C.F., Onukwuli, O.D., 2017. Optimal factor evaluation for the dissolution of alumina from azaraegbelu clay in acidic solution using RSM and ANN comparative analysis. South Afr. J. Chemi. Eng. 43–54.
Okeleye, A.S., Betiku, E., 2019. Kariya (Hildegardia barteri) seed oil extraction: comparative evaluation of solvents, modeling and optimization techniques. Chem. Eng. Commun. 206, 1181–1198.
Oladipo, B., Betiku, E., 2019. Process optimization of solvent extraction of seed oil from *Moringa oleifera*: an appraisal of quantitative and qualitative process variables on oil quality using D-optimal design. Biocatal. Agric. Biotechnol. 20, 101187.
Onoji, S., Iyuke, S., Igbafe, I.A., Daramola, O.M., 2017. *Hevea brasiliensis* (rubber seed) oil: modelling and optimization of extraction process parameters using response surface methodology and artificial neural network techniques. Biofuels 6, 1–15.
Paul, A., Ropo, O., Betiku, E., 2019. Optimization of microwave assisted solvent and extraction on non-edible Sandbox (*Hura crepitans*) seed oil: a potential biodiesel feedstock. Renew. Energy 141, 349–358.
Ropo, O., Paul, A., Sotunde, B., Betiku, E., 2020. Process Modeling of Solvent Extraction of Oil from Hura Creptans Seeds: Adaptive Neuro-Fuzzy Inference System versus Response Surface Methodology: Biomass Conversion and Biorefinery.
Shut, S.H., Lee, K.L., Kamaruddin, A.H., Tusup, S., 2010. Reactive extractions of *Jatropha curcas* seed for production of biodiesel; Process optimization study. Environ. Sci. Technol. 44, 4361–4367.
Statista, 2020. Palm Oil: Global Production Volume, 2012/13-2020/21. www.statista.com.
Topallar, H., Gecgel, U., 2000. Kinetic and thermodynamics of seeds in the presence of aqueos acidic hexane solutions. Turk. J. Chem. 24, 247–253.
Tsakins, J., Gergis, L.V., Dourtoglou, V., Spiliotus, V., 1999. Characterization of *Moringa olifera* variety mbololo seed oil of Kenya. J. Agric. Food Chem. 47, 4495–4499.
Uzoh, C.F., Onukwuli, O.D., 2016. Extraction, analysis and desaturation of gmelina seed oil using different soft computing approaches. S. Afr. J. Chem. Eng.
Zainudin, A., Asyraf, A., Mustafa, M., 2016. The Likert scale analysis using parametric based Structural Equation Modeling (SEM). Comput. Methods Soc. Sci. 4 (1), 13–21.